Transfer of Long-Chain Fluorescent Free Fatty Acids between Unilamellar Vesicles†

Judith Storch and Alan M. Kleinfeld*
Department of Physiology and Biophysics, Harvard Medical School, Boston, Massachusetts 02115
Received August 9, 1985

ABSTRACT: Movement of free fatty acids (ffa) between small unilamellar vesicles (SUV) was studied by measuring the transfer of fluorescent *n*-(9-anthroyloxy)-labeled analogues (AOffa) between donor and acceptor vesicles. Donors were composed of egg phosphatidylcholine (PC) loaded with 1–2 mol % AOffa, and acceptors were egg PC containing 10–12 mol % *N*-(7-nitro-2,1,3-benzoxadiazol-4-yl)phosphatidylethanolamine (NBD-PE). The fluorescence of AO added directly to acceptor SUV was >98% quenched by energy transfer to NBD. Thus, AOffa movement from donor to acceptor was monitored by the time-dependent decrease in AO fluorescence. The transfer of the short-chain AOffa, although too fast to be resolved by the methods used here, is consistent with studies that find transfer rates on the order of milliseconds and kinetics which are first order. In contrast, transfer rates for the long-chain AOffa are more than 2 orders of magnitude slower, and the kinetics of the transfer process are best described by the sum of two exponentials plus a constant. The ffa ionization state was also found to be an important determinant of transfer rate. The charged species transferred an average of 10-fold faster than the protonated ffa. The ffa pK_a in the membrane is 9, as calculated from the pH dependence of transfer. Similar to results found for other lipids, long-chain AOffa are transferred via water rather than a collision-mediated process. The aqueous phase route of AOffa intermembrane transfer is indicated by the lack of effect on transfer of large alterations in the product of donor and acceptor phospholipid concentrations. Moreover, the transfer rate is decreased as [NaCl] is increased from 0.1 to 4 M. This effect of ionic strength is probably due not only to a decrease in the aqueous phase partition of the AOffa but also to an alteration in bilayer structure, as measured by fluorescence polarization of 1,6-diphenyl-1,3,5-hexatriene. The observed kinetics are consistent with a model in which the transfer involves two steps: transbilayer movement between the inner and outer bilayer leaflets, followed by transfer from the outer leaflet to the aqueous phase (off rate). Within the framework of this model, the observed slow rate is primarily determined by the rate of transbilayer movement, and the observed fast rate is approximately equal to the off rate. The off rate is about 10-fold faster than the rate of transbilayer movement.

Free fatty acids (ffa)[1] are the primary energy source for skeletal and heart muscle. An essential step in energy utilization is movement of the ffa from its adipocyte storage site to these target cells, a process which involves transfer across two membranes. Transmembrane movement of ffa is also a necessary step in gastrointestinal lipid absorption, and there is considerable physiological evidence that acyl chain length is a major factor governing intestinal transport of ffa (Carey et al., 1983).

While it is generally believed that fatty acid transfer across membranes occurs by diffusion through the lipid bilayer, several lines of evidence suggest that the process may be protein mediated as well as chain-length dependent. Two distinct transport mechanisms for short- and long-chain ffa have been described in *Escherichia coli* (Nunn et al., 1979; Maloy et al., 1981). The short-chain ffa are taken up via diffusive transport, while long-chain ffa uptake is saturable, and a 33-kDa inner membrane protein has been identified as the gene product responsible for long-chain ffa transport (Ginsburgh et al., 1984). Protein-mediated saturable uptake of long-chain ffa appears to occur in the adipocyte as well, where transport has been shown to be irreversibly inhibited by micromolar concentrations of 4,4′-diisothiocyanostilbene-2,2′-disulfonate (DIDS; Abumrad et al., 1984). Recently, Stremmel et al. (1985) have described the saturable binding of [^{14}C]oleic acid to a 40 000-dalton integral plasma membrane protein in rat intestinal microvillus membrane. Although these studies indicate that the uptake of lcffa into cells is complex, no studies have been carried out which examine the transfer of lcffa between membranes in a pure lipid system.

The present studies were undertaken in order to examine the transfer of ffa between model lipid vesicles. Previous studies have focused only on short-chain ffa. Sengupta et al. (1976) reported that the intermembrane exchange kinetics of a fluorescent analogue of decanoic acid (10:0) were first order and could be slowed by addition of cholesterol. Doody et al.

† This work was supported by a grant-in-aid from the American Heart Association with funds contributed in part by the Massachusetts Affiliate (83-789) and by Grant PCM-830268 from the National Science Foundation (both to A.M.K.). This work was done during the tenure of an Established Investigatorship of the American Heart Association, with funds contributed in part by the Massachusetts Affiliate (82-174, to A.M.K.), and during the tenure of a research fellowship from the American Heart Association, Massachusetts Affiliate (13-409-834, to J.S.).

[1] Abbreviations: AOffa, *n*-(9-anthroyloxy) free fatty acid; CF, 5-(6)-carboxyfluorescein; ffa, free fatty acid(s); lcffa, long-chain ffa; scffa, short-chain ffa; PC, phosphatidylcholine; SUV, small unilamellar vesicle(s); DPH, 1,6-diphenyl-1,3,5-hexatriene; NBD-PE, *N*-(7-nitro-2,1,3-benzoxadiazol-4-yl)phosphatidylethanolamine; kDa, kilodalton(s); DIDS, 4,4′-diisothiocyanostilbene-2,2′-disulfonate; TLC, thin-layer chromatography; Tris, tris(hydroxymethyl)aminomethane; DPPC, dipalmitoylphosphatidylcholine; DMPC, dimyristoylphosphatidylcholine; 11AU, 11-(9-anthroyloxy)undecanoic acid; 12AD, 12-(9-anthroyloxy)dodecanoic acid; 2- and 16AP, 2- and 16-(9-anthroyloxy)palmitic acid; 2-, 3-, 6-, 9-, 10-, and 12AS, 2-, 3-, 6-, 9-, 10-, and 12-(9-anthroyloxy)stearic acid; 12AO, 12-(9-anthroyloxy)oleic acid.

0006-2960/86/0425-1717$01.50/0

(1980) studied the kinetics of transfer of a fluorescent analogue of nonanoic acid (9:0) between small unilamellar vesicles (SUV). They demonstrated that transfer proceeds through the aqueous phase and that transbilayer movement ("flip-flop") is not rate limiting for the transfer process. Recently, Wolkowicz et al. (1984) reported that the transfer rate of pyrenyldodecanoic acid (12:0) is first order and decreases as vesicle size increases.

In order to compare the transfer kinetics of long-chain ffa (16 and 18 carbons) and short-chain ffa, we have developed a simple system for directly monitoring the transfer of fluorescent fatty acid analogues between donor and acceptor lipid vesicles. In comparison to the use of radiolabeled ffa, rapid transfer can be monitored since donor and acceptor vesicles need not be physically separated in order to determine the extent of transfer. Our results demonstrate that the transfer of long-chain ffa is markedly slower than short-chain ffa transfer. Moreover, the mechanism of transfer of long-chain ffa between phospholipid membranes is complex, and the process can be regulated by properties of the membrane bilayer, the aqueous phase, and the ffa itself.

Materials and Methods

Materials. 5-Carboxyfluorescein (CF) and the following series of 9-anthroyloxy-labeled fatty acids were obtained from Molecular Probes (Junction City, OR): 11-(9-anthroyloxy)-undecanoic acid (11AU); 12-(9-anthroyloxy)dodecanoic acid (12AD); 2- and 16-(9-anthroyloxy)palmitic acid (2AP and 16AP); 2-, 3-, 6-, 9-, 10-, and 12-(9-anthroyloxy)stearic acid (2-, 3-, 6-, 9-, 10-, and 12AS); and 12-(9-anthroyloxy)oleic acid (12AO). Thin-layer chromatography of the AO probes with a solvent system of chloroform/hexane/methanol (5:5:1 v/v; Thulborn et al., 1978) showed a major and several minor fluorescent bands. The major band was scraped off and the fluorophore eluted with chloroform. Transfer rates measured either with the purified probe or with the starting material showed no apparent differences, and probes were therefore routinely used without further purification. *N*-(7-Nitro-2,1,3-benzoxadiazol-4-yl)phosphatidylethanolamine (NBD-PE) was from Avanti Biochemicals (Birmingham, AL). 1,6-Diphenyl-1,3,5-hexatriene (DPH) was purchased from Aldrich Chemical Co. (Milwaukee, WI). Egg phosphatidylcholine (egg PC) and cholesterol were from Sigma (St. Louis, MO). Lipid stock solutions and vesicles were periodically monitored for the presence of lysophospholipids and/or ffa by TLC, using a modification of the two-stage development system described by Ando et al. (1980), as previously described (Storch & Schachter, 1985).

Vesicle Preparations. Except where noted, all vesicles were prepared from 99+% pure L-α-phosphatidylcholine. Small unilamellar vesicles (SUV) were prepared as described by Huang and Thompson (1974). Stock solutions of lipid, stored at −20 °C in chloroform, were mixed thoroughly in a round-bottom flask, dried with a rotary evaporator, and lyophilized overnight to ensure removal of trace organic solvent. Buffer was added, and the mixture (typically 8 mM phospholipid) was sonicated for 50 min at 4 °C under nitrogen using a Branson sonicator set at 70 W. Titanium particles and any remaining large multilamellar vesicles were removed by centrifugation at 105000*g* for 45 min. Several SUV preparations were run on a Sepharose 4B gel filtration column (Pharmacia Fine Chemicals, Piscataway, NJ). In no case was lipid detected in the void volume, showing that ultracentrifugation had indeed removed large vesicles. The standard buffer was 40 mM Tris/100 mM NaCl at pH 8.1. Acetate buffer was used for the pH range 3–5 and Tris for the pH range 6–10. Phospholipid concentration was determined as inorganic phosphate according to the Gomori (1942) method.

For experiments designed to measure the transmembrane distribution of AOffa, CF was trapped inside SUV during sonication, and vesicles were chromatographed on a Sephadex G-25 column to remove untrapped fluorophore. The column eluent was monitored by measuring CF fluorescence at 520 nm (excitation 493 nm), and light scattering at 350 nm and/or [^{14}C]DPPC tracer phospholipid was used to assay SUV. A vesicle peak coincident with CF fluorescence was observed in the void volume and was well separated from untrapped CF. The concentration of the trapped CF was equal to that of the solution (20–35 mM) used during sonication, as determined by an estimation of the internal SUV volume of 0.17 μL/μmol of phospholipid (Enoch & Strittmatter, 1979) and the absorbance ($\epsilon \sim 70\,000$ M^{-1} cm^{-1}). To assure that the CF associated with the SUV peak was in fact trapped, an increase in fluorescence (resulting from a decrease in self-quenching) was observed upon addition of 0.5% Triton X-100. CF did not adhere to the vesicle surface since, upon addition of preformed SUV to a CF solution followed by G-25 chromatography, no CF fluorescence was found to be coincident with the SUV peak.

Incorporation of AOffa Probes. Donor SUV were loaded with probe either by addition of the fluorophore to preformed vesicles or by cosonication of probe with lipid. To incorporate probes into preformed SUV, a concentrated stock solution of probe in ethanol was added while vortex mixing. Typically, a 3-μL aliquot of a 1.5 mM stock solution was added to 4.8 mL of 0.05 mM SUV to give 1.9 mol % AOffa and a final ethanol concentration of <0.1%. Vesicles were incubated with probe at room temperature for a minimum of 45 min. These SUV are designated "outside loaded", and this method of incorporation was utilized unless otherwise noted. Alternatively, probe was incorporated into SUV during sonication by thoroughly mixing the stock probe with lipid in organic solvent, and these vesicles are designated "sonication loaded".

Fluorescence Measurements. Fluorescence intensity measurements were made with a Perkin-Elmer MPF-2A fluorescence spectrophotometer. Excitation and emission slits were 6 and 7 nm, respectively. Measurements were carried out in 3-mm path-length microcuvettes containing 0.25–0.35 mL of solution. Excitation was at 383 nm, and emission was monitored at 450 nm. A constant temperature of 24 °C was maintained with a circulating bath.

AOffa Transfer Assay. Donor vesicles of egg PC were loaded with 1 or 2 mol % AOffa as described previously. Acceptor vesicles were prepared by sonication of egg PC and 12 mol % NBD-PE. The efficiency of quenching by the acceptor vesicles was determined by adding AOffa directly to these vesicles. Greater than 98% quenching of AO emission was observed for all probes and was independent of pH between pH 3 and pH 11. Fluorescence intensity of the AOffa probes in buffer was negligible at the concentrations used in our assay.

In a typical transfer assay, equal volumes of donor and acceptor vesicles were vortex mixed, resulting in final phospholipid concentrations of 0.025 and 0.5 mM for the donor and acceptor, respectively. The reaction mixture was quickly transferred to a microcuvette, and the first measurement was made at 30 s. Similar transfer kinetics were observed when a rapid-stirring device (~10-s mixing time) was used to mix the donors with acceptors (Kleinfeld et al., 1979). Depending upon the probe used, transfer kinetics were monitored by measuring the intensity between 30 s and 2 h. The NBD-PE

Table I: Kinetic Analysis of Long-Chain AOffa Transfer Data[a]

AOffa	n	k_{fast} (min^{-1})	A_{fast}	k_{slow} (min^{-1})	A_{slow}	C	k_{av} (min^{-1})
2AP (16:0)	9	2.6 ± 0.7	0.34 ± 0.04	0.14 ± 0.02	0.56 ± 0.03	0.10 ± 0.01	1.07
2AS (18:0)	13	1.4 ± 0.3	0.30 ± 0.03	0.03 ± 0.01	0.48 ± 0.03	0.22 ± 0.03	0.56
12AS (18:0)	3	2.4 ± 0.9	0.33 ± 0.08	0.39 ± 0.06	0.59 ± 0.08	0.06 ± 0.09	1.11
12AO (18:1)	3	2.8 ± 0.3	0.79 ± 0.04	0.18 ± 0.10	0.11 ± 0.03	0.06 ± 0.09	2.50

[a] The data were fitted to eq 2 to obtain A_{fast}, k_{fast}, A_{slow}, and k_{slow}. k_{av} is a weighted average of the two components (eq 3). Donor and acceptor concentrations were 0.025 and 0.5 mM, respectively. Values shown are mean ± SD for n separate determinations.

in the acceptor is nonexchangeable (Monti et al., 1978). The total fluorescence was monitored by measuring the intensity of donor vesicles added to acceptor vesicles without the quencher and did not change over the time course of the experiment.

Data Analysis. Intensities at each time point were determined as the peak height at 450 nm from which was subtracted the intensity due to scatter from vesicles without probe. A correction for the inner filter due to NBD absorbance at 450 nm was applied since the total fluorescence intensity is determined without NBD. In a typical experiment with 0.06 mM NBD, this multiplication factor was 1.5. The percent of probe remaining in the donor vesicles was evaluated by dividing the corrected intensity by the total fluorescence.

The variation of fluorescent intensity with time was analyzed by fitting the observed intensities to the function

$$F(t) = \sum_i A_i \exp(-k_i t) + C \quad (1)$$

The fits were performed by using a nonlinear least-squares procedure based upon the Marquart algorithm (Bevington, 1969). Fit quality was assessed by the normalized χ^2 with standard deviations of the intensities (determined by multiple sampling) of <2%. In all cases, the χ^2 obtained with a single exponential was at least 10-fold larger than with two exponentials. For two exponentials, the normalized χ^2 values were generally less than or equal to 1. Thus, in all measurements, the kinetics could be satisfactorily described by

$$F(t) = A_{fast} \exp(-k_{fast} t) + A_{slow} \exp(-k_{slow} t) + C \quad (2)$$

Figure 1 illustrates the difference between a one- and two-exponential fit for a typical measurement. The average transfer rate (k_{av}) was calculated as the sum of the amplitude of a component multiplied by its rate:

$$k_{av} = \sum_{i=1}^{2} A_i k_i / \sum_{i=1}^{2} A_i \quad (3)$$

DPH Polarization. Steady-state fluorescence polarization of DPH was measured by using an SLM 4800 spectrofluorometer as described in Matayoshi and Kleinfeld (1981).

Results

Effect of ffa Chain Length. Transfer of the *n*-(9-anthroyloxy) fatty acids between donor and acceptor egg PC SUV was monitored at 24 °C. The time resolution of the assay was not sufficient to accurately measure the transfer of two short-chain AOffa probes, 11AU (11:0) and 12AD (12:0). The rapid transfer of short-chain AOffa is consistent with the rates reported for pyrenyl-9:0 (Doody et al., 1980) and pyrenyl-10:0 (Sengupta et al., 1976), which had half-times at room temperature of 0.2 and 3.3 s, respectively. For comparative purposes, a rough estimation from our data for 11AU yields a half-time of less than 2 s.

In contrast, the transfer of most long-chain AOffa (16 and 18 carbons) is between 1 and 2 orders of magnitude slower than 11AU. Even the long-chain probe which transfers most rapidly, 16AP, has an average rate which is a minimum of 5-fold slower than that for 11AU. Figure 1 shows a comparison of typical transfer kinetics of 12AD and 12AS. The other major difference between short- and long-chain ffa transfer, as shown in Figure 1, is that the transfer process for the long-chain ffa analogues is described by two rates plus a constant amount of probe remaining with the donor vesicle at equilibrium. Short-chain ffa transfer, on the other hand, is apparently monoexponential (Sengupta et al., 1976; Doody et al., 1980).

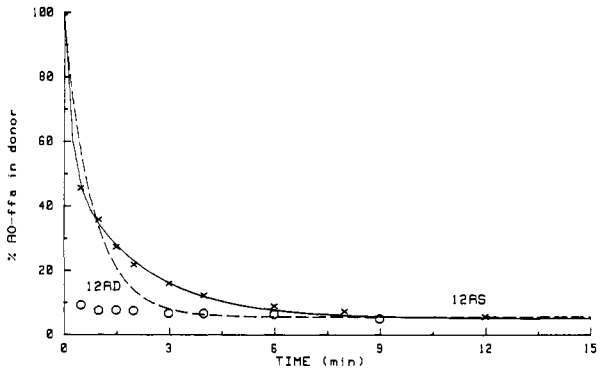

FIGURE 1: Transfer of AOffa between SUV. Donors (0.025 mM) containing 2 mol % of the short-chain 12AD (○) or long-chain 12AS (×) were mixed with a 20-fold excess of acceptors at 24 °C and pH 8.1. Kinetics of the 12-carbon 12AD are too rapid to resolve (equilibrium is reached by the first time point at 30 s). For the 18-carbon 12AS, the time dependence of donor fluorescence was fitted with a function equal to a sum of exponentials plus a constant: the data are best described by a two-component fit (—; $\chi^2 = 0.21$); the fit to a single component (- - -; $\chi^2 = 6.13$) is also shown.

Effects of chain length are also illustrated by a comparison of the transfer rate constants for 2AS (18:0) and 2AP (16:0), as shown in Table I. For both probes, the k_{slow} accounts for the larger part of total transferred ffa. The slow component of 2AS transfer (0.03 min^{-1}) is approximately 5-fold slower than that of 2AP (0.14 min^{-1}). Given the 20-fold excess of acceptor over donor phospholipid, the expected constant value of eq 1 (C), corresponding to equilibrium, should be 0.05. As Table I shows, the values for 2AP and 2AS were 0.10 and 0.22, respectively. This deviation from the expected equilibrium value is only observed for 2AS and 2AP. All other derivatives exhibit plateau values of 0.06 ± 0.02. Thus, for reasons which are not clear, 2AS and 2AP exhibit a third pool of AOffa whose transfer is so slow as to appear unchanging within the uncertainty of our measurements.

Fatty Acid Unsaturation. The effect of acyl chain unsaturation on fatty acid transfer was studied by comparing the kinetics of 12-(9-anthroyloxy)stearate and 12-(9-anthroyloxy)oleate. As seen in Table I, the average transfer rate is 2-fold greater for oleate than for stearate. The major difference between the two species is that A_{fast} is 0.33 for 18:0 and 0.79 for 18:1, although k_{slow} is actually greater for 12AS (0.4 min^{-1}) than for 12AO (0.2 min^{-1}).

Effect of pH. To examine the role of ionization state on long-chain ffa intermembrane movement, the transfer of four AOffa was studied as a function of pH, and results are shown in Figure 2. While no consistent change was detected in A_{fast} or k_{fast}, k_{slow} was slowest at low pH and fastest at high pH

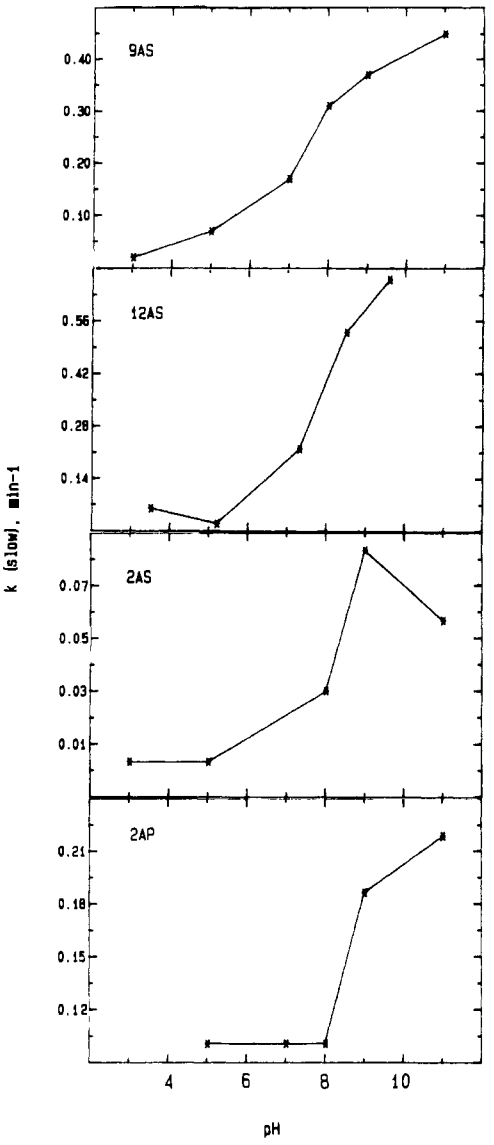

FIGURE 2: pH dependence of k_{slow} for transfer of four long-chain AOffa between SUV. Aliquots of concentrated SUV prepared in pH 8.1 buffer were loaded with AOffa and diluted into appropriate pH buffer immediately prior to the transfer assay. Conditions, except for pH, were as described in Figure 1 and under Materials and Methods.

values, presumably reflecting the protonated and ionic species, respectively. The values of k_{slow} for the ionized forms of the ffa are on the average 10 times those for the protonated forms. For all probes examined, the apparent pH midpoint for transfer occurred at approximately pH 8. No hydrolysis of phospholipid was detected by thin-layer chromatography within the pH range of maximum rate change.

Concentration of AOffa. It has been suggested that ffa may form clusters within the membrane (Hauser et al., 1979). To examine whether clusters could influence the transfer kinetics, measurements were carried out with probe concentrations between 0.5 and 20 mol %, since cluster formation should be sensitive to the probe concentration in the donor vesicle. The results (data not shown) demonstrated that variation of donor 12AS over this concentration range had virtually no effect on the transfer kinetics and therefore the AOffa probably transfer as monomers.

Donor Cholesterol. Cholesterol has been shown to decrease the permeability of phospholipid membranes to glucose, glycerol, water, ions, and hydrophobic anesthetics (Phillips, 1972; Demet et al., 1972; Van Deenen, 1975; Miller & Yu, 1977) and thus might be expected to alter ffa transfer as well.

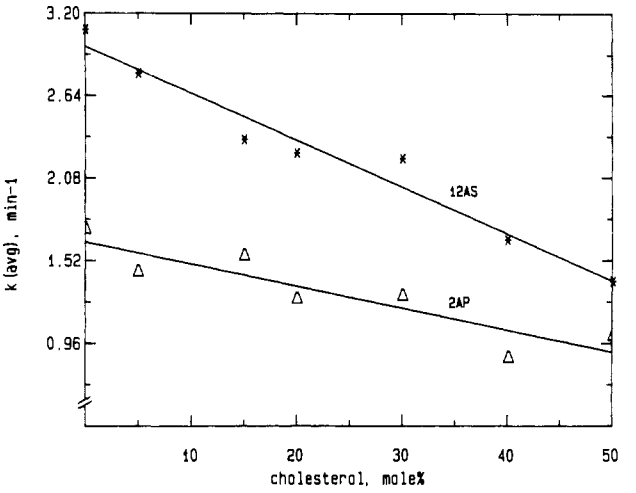

FIGURE 3: Effect of donor cholesterol content on AOffa transfer. Donors were prepared by cosonication of egg PC and cholesterol and were loaded with 12AS (×) or 2AP (△) as described under Materials and Methods. Transfer was measured at 24 °C and pH 8.1.

Transfer rates, therefore, were measured for 2AP and 12AS in egg PC SUV prepared with up to 50 mol % cholesterol. As shown in Figure 3, the average transfer rate for the probes decreased with increasing cholesterol. The effect of cholesterol was different for the two ffa derivatives. With increasing cholesterol, k_{fast} for 2AP decreased by about 50% while k_{slow} was essentially unchanged. For 12AS, both k_{slow} and k_{fast} decreased by about a factor of 2. Virtually no changes in A_{fast} and A_{slow} were observed.

Effect of Phospholipid Concentration on 12AS Transfer. Spontaneous transfer of ffa between vesicles can occur either through the aqueous phase or by a vesicle collision-mediated exchange. If transfer is collision-mediated, then the rate should display a first-order increase with the acceptor vesicle concentration. To examine this possibility, the rate of 12AS transfer was measured for constant donor concentration and varying donor:acceptor ratios. The rate of transfer was found to be essentially unchanged (data not shown) by alteration of the donor to acceptor phospholipid ratio between 1:4 and 1:160.

Ionic Strength. The effect of ionic strength on transfer was studied to determine the influence of aqueous phase solubility on probe movement. Increasing ionic strength caused a logarithmic decrease in the rates of both k_{fast} and k_{slow} of 12AS and 16AP (Figure 4). For both probes, 4M NaCl increased the transfer half-times of both components by approximately 2 orders of magnitude compared to 0.1 M NaCl. Although these results seem to support aqueous phase solubility as an important factor in the process, it is possible that at least part of this effect might be due to alterations in vesicle structure with ionic strength. To examine this possibility, the fluorescence polarization of DPH in SUV was measured as a function of [NaCl], and the results in Figure 4 (insert) show an increase in polarization (a decrease in lipid motional freedom) as ionic strength is increased.

Effect of Probe Loading. To determine whether transbilayer movement ("flip-flop") of the AOffa from inner to outer leaflet might account for the observed biexponential transfer process, transfer was measured from donor SUV loaded with ffa during sonication or from donors in which the ffa were added to preformed SUV and incubated for 2, 5, or >45 min. The transfer kinetics from these two vesicle populations were virtually identical when incubated for 5 or >45 min. In the case of the 2-min incubation, however, a small but reproducible increase in A_{fast} was observed, with k_{fast} and k_{slow} remaining unaffected.

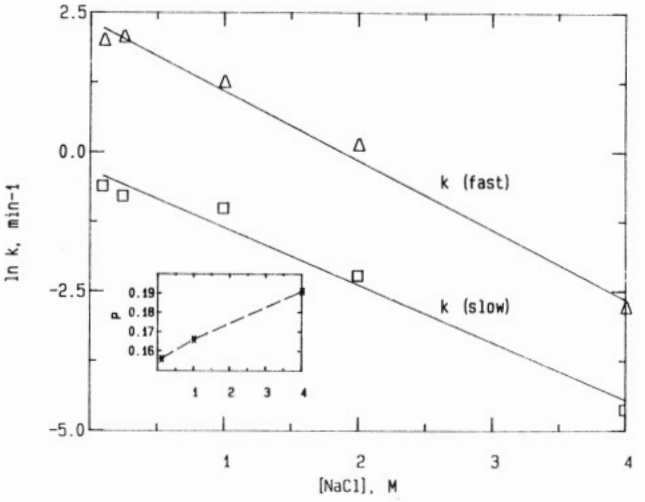

FIGURE 4: Effect of ionic strength on 16AP transfer. Aliquots of concentrated SUV prepared in 0.1 M NaCl/Tris buffer were loaded with 16AP and diluted 10-fold into the appropriate high-NaCl buffer prior to the transfer assay. Conditions, except for [NaCl], were as described under Materials and Methods. Insert: Effect of [NaCl] on DPH polarization in egg PC SUV. Vesicles were 0.2 mM egg PC and contained 2 μM DPH. Measurements were taken at 24 °C. Values shown are the means of two separate preparations.

Table II: Transfer Kinetics from Donors with Trapped CF[a]

		observed		theory	
AOffa	CF	A_{fast}	A_{slow}	Z_4	Z_3
2AP	−	0.42	0.51	0.42	0.51
	+	0.52	0.42	0.54	0.37
12AS	−	0.51	0.45	0.51	0.45
	+	0.62	0.35	0.58	0.37

[a] Values of the preexponential factors A_{fast} and A_{slow} were measured with control vesicles (−) and vesicles containing 35 mM trapped CF (+). The theoretical values were calculated by using Z_3 and Z_4 from eq A13 modified for quenching of AO by CF due to resonance energy transfer.

Flip-flop can also be measured in vesicles which have an initially (t = 0) asymmetric AOffa distribution (see below for initial distribution). An asymmetric distribution can be simulated by adding the AOffa to vesicles containing CF trapped inside. Since CF serves as a resonance energy transfer acceptor from AO with an R_0 of about 35 Å, there will be greater quenching of the AOffa in the inner vs. the outer hemileaflet of the vesicles. Transfer measurements of 2AP, 2AS, and 12AS were carried out with vesicles in which 35 mM CF was trapped, and the results, shown in Table II, indicate that A_{fast} increases and A_{slow} decreases in comparison to donors without CF.

CF-containing vesicles were also used to determine the initial AOffa transmembrane distribution. In these measurements, AO probes were added to the outside of SUV prepared with 20 mM 5-carboxyfluorescein trapped inside, and to control vesicles with no CF. Energy transfer efficiency was determined as $1 - I(CF)/I(C)$ where $I(CF)$ and $I(C)$ are the AO emission in CF-trapped and control vesicles, respectively. Table III compares the measured values with the values predicted for probe entirely in the outer leaflet or uniformly distributed between both leaflets. These predicted values were calculated by using methods similar to those of Shaklai et al. (1976) for transfer from a two-dimensional array of the AOffa to CF uniformly distributed within the internal aqueous region of the SUV. These results demonstrate that probe is indeed distributed in both inner and outer hemileaflets.

Effect of Vesicle Size. To test whether the observed biexponential transfer kinetics were due to vesicle size heterogeneity, the Sepharose 4B SUV peak was subdivided into three fractions, and 12AS transfer was measured from these different size donors. [The typical size range for an SUV peak is approximately 195–230 Å (Huang & Thompson, 1974).] Although the average transfer from the largest vesicles was about 15% slower than the smallest, the kinetics from all three subfractions were biexponential.

Table III: Initial Distribution of AOffa between Inner and Outer Hemileaflets of SUV As Determined by 5-Carboxyfluorescein Quenching[a]

	% quenching by trapped CF		
		theory	
AO attachment site	measured	both leaflets	outer only
2-	0.37	0.31	0.12
12-	0.53	0.44	0.36
16-	0.54	0.45	0.41

[a] SUV containing trapped 5-carboxyfluorescein (20 mM) were prepared as described under Materials and Methods and incubated with AOffa for >45 min at room temperature. The degree of quenching was determined relative to control SUV (no CF trapped), and values were compared with theoretical calculations for the probe entirely in the outer leaflet or distributed 2:1 outer:inner, on the basis of the 2:1 phospholipid ratio between SUV hemileaflets.

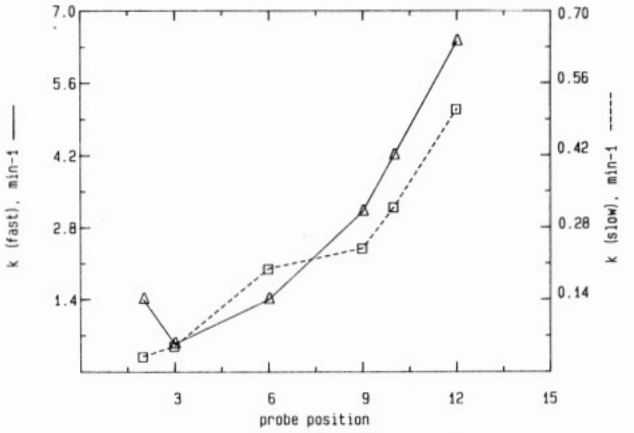

FIGURE 5: Effect of probe attachment site on transfer rates. Transfer of the (9-anthroyloxy)stearate derivatives, with the fluorescent moiety attached at n = 2–12, was measured as described under Materials and Methods. (—) k_{fast}; (- - -) k_{slow}.

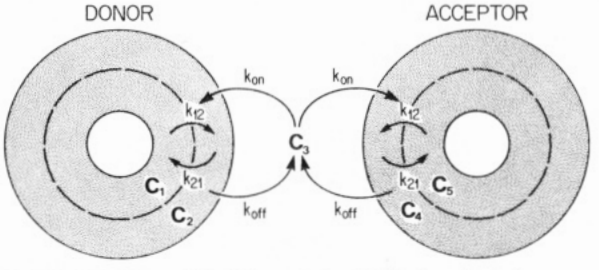

FIGURE 6: Kinetic model of long-chain AOffa transfer between egg PC SUV. The concentrations of the AOffa as a function of time in each of the five regions are $C_1(t)$ for the inner leaflet of the donor, $C_2(t)$ for the outer donor leaflet, $C_3(t)$ for the aqueous phase, and $C_4(t)$ and $C_5(t)$ for the outer and inner acceptor leaflets, respectively. k_{12} is the transfer rate from inner to outer hemileaflet, k_{21} the reverse rate, and k_{off} the rate of transfer from the outer leaflet to the aqueous phase. k_{on}, the rate of transfer from the aqueous phase to the outer leaflet, is a bimolecular rate given in units of $(min \cdot mol)^{-1}$.

Effect of AO Position on Transfer. To determine the effect of AO attachment site on transfer kinetics, measurements were carried out with the 2-, 3-, 6-, 9-, 10-, or 12-stearic acid derivatives. The results shown in Figure 5 demonstrate that the average transfer rate increases as the distance increases from the carboxy terminal. Both the fast and slow components

increase monotonically with attachment site (Figure 6), and the average rate increases from 0.56 min^{-1} for 2AS to 2.5 min^{-1} for 12AS. Similar behavior is observed for the 16:0 analogues. The slowly transferring component has a rate constant of 0.14 min^{-1} as compared to 0.61 min^{-1} for 2AP and 16AP, respectively, and average rates are 1.1 and 6.2 min^{-1}, respectively.

Discussion

This work examines the spontaneous transfer of AO-labeled free fatty acids between small unilamellar vesicles and is the first study of long-chain (16 and 18 carbons) ffa transfer in a model lipid system. The results demonstrate that (1) transfer occurs through the aqueous phase, (2) the transfer of the short-chain AOffa is consistent with studies that find transfer rates on the order of milliseconds and kinetics which are first order, and (3) the transfer rates for the long-chain ffa are more than 2 orders of magnitude slower than for the short-chain ffa and the kinetics of the transfer process are best described by two exponentials. Before these results are discussed in greater detail, a kinetic model will be presented which provides a useful framework to describe the various factors affecting the kinetics.

As seen in Figure 6, the model proposed for the transfer of a long-chain ffa involves five separate regions. The concentrations of the ffa in each region, relative to the bulk solution, as a function of time are designated $C_1(t)$ for the inner leaflet of the donor vesicles, $C_2(t)$ for the outer donor leaflet, $C_3(t)$ for the aqueous phase, $C_4(t)$ for the outer leaflet of the acceptor, and $C_5(t)$ for the inner acceptor leaflet. The differential equations which relate these concentrations to the appropriate rate constants and the vesicle concentrations are given by

$$dC_1(t)/dt = k_{21}C_2(t) - k_{12}C_1(t) \quad (4)$$

$$dC_2(t)/dt = k_{12}C_1(t) + k_{on}[D]C_3(t) - k_{21}C_2(t) \quad (5)$$

$$dC_3(t)/dt = k_{off}[C_2(t) + C_4(t)] - k_{on}[T]C_3(t) \quad (6)$$

$$dC_4(t)/dt = k_{12}C_5(t) + k_{on}[A]C_3(t) - k_{21}C_4(t) \quad (7)$$

$$dC_5(t)/dt = k_{21}C_4(t) - k_{12}C_5(t) \quad (8)$$

in which [D], [A], and [T] are the concentrations of the donor, acceptor, and total donor plus acceptor vesicles, respectively, k_{12} is the transfer rate from the inner to the outer leaflet, k_{21} is the reverse rate, k_{off} is the rate of transfer from the outer leaflet to the aqueous phase, and k_{on} is the bimolecular rate for transfer from the aqueous phase to the outer leaflet. With the exception of k_{on}, the rate constants are in units of min^{-1}, whereas k_{on} is $(min\ M)^{-1}$. The equality of donor and acceptor rate constants is warranted since, with the exception of 12% NBD-PE, the acceptors are identical with the donor vesicles.

This model is similar to the one used by Arvinte and Hildenbrand (1984) to describe the transfer of NBD-dilauroyl-PE between SUV. Their model, in turn, was based upon the studies of Nakagawa (1974), Thilo (1977), and Nichols and Pagano (1981). A common thread in all these studies was the assumption that the steady state is reached rapidly in the aqueous phase [$dC_3(0)/dt = 0$]. In addition, Arvinte and Hildenbrand (1984) solved eq 4–8 by fixing the relationship between k_{12} and k_{21} ($k_{12} = 2k_{21}$). To fully explore these assumptions, a solution independent of these restrictions is necessary. The solution to this formidable problem was obtained by using the symbolic manipulation program MACSYMA and is given in the Appendix. As shown in the Appendix, the rapid equilibrium approximation for C_3 is, in fact, valid for reasonable values of the rate constants, and, therefore, return flux does not contribute significantly to the observed kinetics.

Although the general solution for this model is fairly complex, considerable simplification occurs for the rate constants encountered in lipid exchange kinetics. Thus, except for the unlikely occurrence of extremely slow k_{on} rates [<10 $(min\ M)^{-1}$], only the magnitude of the preexponential factors of the second two terms of eq A4 and A5 is significant, and, therefore, the predicted kinetics will be biexponential plus a constant, the latter being the equilibrium concentration. Moreover, the exponent of the term A_{slow} is, to a first approximation, a function only of k_{12} and k_{21}, and the exponent of A_{fast} is approximately equal to k_{off}.

This model of the lcffa transfer process is consistent with the observed biexponential behavior arising from transbilayer movement and the off step of the AOffa from the donor outer leaflet. Several other possible experimental factors contributing to such behavior have also been examined. (1) Donor vesicle size heterogeneity might be expected to result in multiexponential kinetics. McLean and Phillips (1984), e.g., have shown that the rate of cholesterol transfer from 230-Å vesicles is 4-fold faster than from 800-Å vesicles. As discussed under Results, however, transfer rates measured with vesicles from the extreme ends of the Sepharose 4B peak differed by less than 15%, and, most significantly, the kinetics of each fraction were biexponential. (2) Small amounts of vesicle collision which might, in some way, contribute to the biexponential kinetics are also ruled out by the absence of any effect of donor or acceptor concentration on the kinetics. (3) As discussed in greater detail below, biexponential kinetics are also independent of the ffa ionization state. (4) Biexponential kinetics resulting from the formation of probe aggregates are also unlikely since the transfer kinetics are unchanged over a 40-fold alteration in donor AOffa concentration.

The most likely basis, therefore, for the observed kinetics is that the rate of transmembrane flip-flop is appreciably slower than the rate at which the ffa monomer dissociates from the outer bilayer leaflet. This hypothesis was tested by comparing the transfer from sonication-loaded vs. outside-loaded donor vesicles, as described under Results. For the latter SUV, incubation was for 2, 5, or >45 min. No differences between the two types of donors were seen with longer incubation times, but the vesicles incubated for 2 min did exhibit a small increase in A_{fast} compared to sonication-loaded vesicles. In addition, as seen in Table II, the transfer kinetics from CF-containing donors reflect a greater contribution from A_{fast} than from vesicles without CF. The values of A_i predicted by the kinetic model were evaluated for donors with and without CF by multiplying $C_1(0)$ and $C_2(0)$ with 1 − transfer efficiency expected for the inner and outer leaflets, respectively. As Table II shows, the results for 12AS and 2AP are in very good agreement with the prediction based on flip-flop.

To analyze the experimental kinetics in terms of the model parameters, the predicted fluorescence intensity was calculated by using only the normalized donor fluorescence according to

$$F(t) = [C_1(t) + C_2(t)]/[C_1(0) + C_2(0)] = Z_3e^{m_3t} + Z_4e^{m_4t} + Z_{eq} \quad (9)$$

since the fluorescence in the acceptor and the aqueous phase is negligible. According to the present model, three rate constants (since the value of k_{21}/k_{12} is not fixed) must be determined in order to evaluate Z_3 and Z_4. Values of k_{off} and k_{12} were determined for particular values of k_{21}/k_{12} by comparing exponents in eq 9 with those in eq 2. The expressions for the rates m_3 and m_4 are given in the Appendix. These values for the rate constants were used to calculate the preexponential factors Z_3 and Z_4 (eq A14 and A15, respectively) as a function of k_{21}/k_{12}.

Table IV: Comparison of Experimental and Model Kinetic Parameters: Effect of Fluorophore Position on Transfer[a]

	observed		model	
AO-18:0	A_{slow}	A_{fast}	Z_4	Z_3
2AS	0.48	0.30	0.64	0.31
3AS	0.57	0.34	0.62	0.34
6AS	0.74	0.21	0.72	0.23
9AS	0.61	0.33	0.62	0.34
10AS	0.60	0.38	0.59	0.36
12AS	0.55	0.38	0.60	0.36

[a] The observed values of k_{fast} and k_{slow} shown in Figure 5 were used to solve for k_{off}, k_{12}, and k_{21} for $k_{21}/k_{12} = 1.0$ by using eq A11 and A12. Z_3 and Z_4 were evaluated by using these rates and eq A14 and A15.

These preexponential factors are the most important reflections of the kinetic model, and therefore, the validity of the model is assessed by comparing Z_3 and Z_4 (eq 9) with A_{slow} and A_{fast} (eq 2). Results of such a comparison demonstrate that the biexponential kinetics of the 16- and 18-carbon AOffa are readily explained by the kinetic model described above. Table IV compares the data for the effect of AO probe position on transfer (Figure 5) with the proposed kinetic model. Preexponential factors Z_3 and Z_4 obtained with k_{21}/k_{12} values ≥ 1 and with k_{off} values about 10-fold greater than k_{12} are in excellent agreement with the observed values A_{slow} and A_{fast}. The model, therefore, predicts that flip-flop is rate limiting and that the flip-flop rate as well as the off rate increase for AO positions deeper in the bilayer. The model also predicts that at $t = 0$ the probe density (relative to the lipid phase) is greater in the inner than in the outer hemileaflet, since the vesicles are SUV (ratio of outer to inner areas ≈ 2) and since for most of the probes $k_{21}/k_{12} \sim 1$. Although this result is somewhat surprising and presumably reflects the structural asymmetry of SUV, it is no more surprising than the requirement of $k_{12} = 2k_{21}$ needed to achieve equal hemileaflet densities.

Effect of ffa Structure on Transfer Kinetics. The most dramatic effects of ffa structure are differences between short-chain and long-chain free fatty acids. The results of the present study with the 11- and 12-carbon AOffa are consistent with previous work although the temporal resolution of the present method is not sufficient to exclude a second component. Average half-times of transfer for the long-chain ffa studied here, on the order of minutes, are nearly 2 orders of magnitude slower than for the short chains. Moreover, the average rate of the 16-carbon 2AP is twice that of the 18-carbon 2AS. The relationship between acyl chain length and intermembrane transfer rate has also been observed for phospholipids (Martin & McDonald, 1976; Massey et al., 1982), and a similar relationship has been found for pyrene analogues of alkanes and alcohols, as well as a series of short-chain pyrenylcarboxylic acids (Pownall et al., 1983).

Fatty acyl cis monounsaturation results in a 2-fold increase in the average transfer rate of the 12-(9-anthroyloxy) 18-carbon probes, although the mode of transfer may be different for the unsaturated ffa, as indicated by differences in the relative amounts of A_{fast} and A_{slow} between saturated and unsaturated AOffa. Similarly, Massey et al. (1982) have reported 3–10-fold increases in the rates of spontaneous intermembrane transfer of pyrene-labeled phospholipids as a result of the presence of a single double bond.

Ionization State of the ffa. As the results in Figure 2 demonstrate, charged ffa undergo far more rapid transfer than do protonated ffa. These effects of pH are similar to results obtained by others (Doody et al., 1980; Pownall et al., 1983) for short-chain ffa transfer. The relationship of rate vs. pH for the scffa, however, shows an apparent midpoint at pH 5 and a calculated pK_a in the membrane of 7, while the long-chain ffa transfer midpoint is at pH 8 and the calculated pK_a is 9. These results may reflect a greater suppression of ionization of the lcffa intercalated in the bilayer. Hauser et al. (1979) report that for native stearic acid, the pK_a for the membrane-bound molecule is approximately 8 and that complete ionization occurs at pH 11. The lower pK_a's observed for the scffa may be due to a different form of association of the scffa with the bilayer. Evidence obtained with the short-chain 11-(9-anthroyloxy)undecanoic acid (11 carbons) (Chalpin & Kleinfeld, 1983) suggests that the anthroyl moiety of 11AU is much more accessible to aqueous phase quenchers than its longer chain counterparts and, therefore, the acyl chain is more superficial to the bilayer surface. The faster intermembrane transfer rate of the scffa may therefore occur because they are less strongly bound to the donor vesicle and, therefore, have less of an energy barrier to dissociation.

Although, as we have indicated, the overall rate of transfer increases with pH, the effects of pH on k_{fast} and k_{slow} are quite different: The slow component increases by more than 10-fold over the pH range tested, while the fast component is virtually constant. Indeed, in terms of the kinetic model, the effect is contrary to what one might expect and implies that it is the rate of flip-flop, rather than the off rate, that is affected by pH. Although unexpected, this result is not without precedence. In studies of short-chain ffa, the transfer rate was also observed to increase with pH (Charlton & Smith, 1982; Doody et al., 1980). Since ionization did not prevent or appreciably slow down the rate of flip-flop, it follows that in these studies as well the charged form of the ffa can readily permeate the membrane.

A number of factors may promote the transbilayer movement of the ionized form of the ffa. First, the barrier to flip-flop may be small compared to that for a bare anion, as a result of the delocalized charge of the ffa carboxylate group plus the appreciable affinity of the acyl chain for the hydrocarbon region of the bilayer. The flip-flop rate may also reflect ffa–phospholipid hydrogen bonding. In the protonated state, the ffa may hydrogen bond to the phosphate of the phospholipid head group, whereas ionization of the carboxyl group would disrupt this interaction, and perhaps because of orientation or distance the interaction with the protonated choline is not significant. Effects of hydrogen bonding have in fact been observed in the transfer of pyrene-labeled phospholipids between recombinants of apoprotein and DMPC (Massey et al., 1981). Although hydrogen bonding might be expected to affect both the off and flip-flop rates, large differences in the magnitude of these rates make it likely that the effect is only seen on the rate-limiting step.

Effects of the Aqueous Phase. Increasing the NaCl concentration of the buffer results in dramatic decreases in 16- and 18-carbon ffa transfer rates. This is generally thought to be a result of decreased aqueous solubility of hydrophobic compounds caused by "structure-making" solutes (Charlton & Smith, 1982). Indeed, the results shown in Figure 4 confirm this expectation and indicate that k_{off} decreases with increasing ionic strength, providing strong evidence that intervesicle transfer of AOffa is via the aqueous phase. The lack of effect on the transfer rate of a large variation in the donor:acceptor phospholipid ratio lends further support for monomer transfer through the aqueous phase since the rate constants observed here exclude collision models (Ferrell et al., 1985). Transfer through the aqueous phase has also been shown for cholesterol

(Backer & Dawidowicz, 1981; McLean & Phillips, 1981), phospholipids (Roseman & Thompson, 1980; Nichols & Pagano, 1981; Arvinte & Hildenbrand, 1984), sphingomyelin (Pownall et al., 1982), and short-chain ffa (Doody et al., 1980).

In addition to the effect on k_{fast}, increasing [NaCl] was also associated with a decrease in k_{slow} (Figure 4). This result suggests that in addition to decreasing the aqueous phase solubility of the ffa, increasing ionic strength may alter the structure of the lipid bilayer. To examine this possibility, the fluorescence polarization of DPH in SUV was determined as a function of [NaCl]. As seen in Figure 4 (insert), the polarization increases with [NaCl], indicating that the lipid acyl chain order has increased and may account, in part, for the decrease in the rate of transbilayer movement.

Effect of the Donor Bilayer. The rate of AOffa transfer is also modified by physical properties of the phospholipid bilayer. Addition of cholesterol to donor membranes results in slower intermembrane transfer rates (Figure 3). Sengupta et al. (1976) also found that the rate of intermembrane transfer of pyrenyldecanoic acid was slowed by donor cholesterol enrichment. The effect of cholesterol is greater for probes with the anthroyloxy group further along the hydrocarbon chain. Cholesterol has been shown to increase the rigidity of C2–C10 methylene groups and leave more distal groups and the terminal methyl group relatively unaffected (Darke et al., 1972; Keogh et al., 1973; Kutchai et al., 1983). Thus, the attachment of the anthroyloxy group at the C12 position may, in the presence of cholesterol, result in a tighter association with the hydrophobic core and therefore a reduced rate of dissociation or transfer.

Use of Fluorescent Analogues of ffa. Intrinsic properties of the ffa, such as chain length, unsaturation, and ionization state, are clearly important in regulating the intermembrane transfer rate. Fluorescent derivatives of ffa and phospholipids have been used to study many membrane-related events, including transfer processes in model membranes (Doody et al., 1980; Wolkowicz et al., 1984) and intracellular lipid traffic (Sleight & Pagano, 1985). The AOffa have also been used as ffa analogues to investigate transfer in biological membranes (Morand et al., 1982) as well as to study intracellular metabolism (Gatt et al., 1980). The absolute values obtained in these as well as our studies must, however, be viewed in light of the covalent modification of the native ffa molecule. The site of attachment of the fluorescent moiety affects the transfer process, and it is observed that the rate decreases as the anthroyloxy group approaches the carboxy terminus (Figure 5). Despite such effects, properties of the fluorescent analogues used here are in fact similar to those of ffa. For example, Brecher et al. (1984) have reported that at pH 4, the transfer of [^{14}C]18:1 from multilamellar egg PC–cholesterol vesicles to fatty acid binding proteins was negligible compared to transfer at pH 8. Thus, while there is little doubt that the presence of a relatively large hydrophobic group imparts properties different from the native ffa, the observed relative relationships are likely to hold for unmodified molecules.

Appendix

A complete solution to the kinetic model represented by eq 3–7 was obtained by using the symbolic manipulation program MACSYMA (Mathlab Group, Laboratory for Computer Science, Massachusetts Institute of Technology, Cambridge, MA 02139). Initial conditions were as follow: (i) a steady state exists among the C_i at time = 0, $dC_1(0)/dt = dC_2(0)/dt = 0$; (ii) the total probe concentration is equal to the sum in regions 1–3, $C_T = C_1(0) + C_2(0) + C_3(0)$; and (iii) $C_4(0) = C_5(0) = 0$. For these conditions, eq 3–5 yield

$$C_1(0) = k_{21}C_2(0)/k_{12} \quad \text{(A1)}$$

$$C_3(0) = k_{on}[D]C_2(0)/k_{off} \quad \text{(A2)}$$

$$C_2(0) = \frac{k_{12}k_{on}[D]C_T}{k_{on}[D](k_{12} + k_{21}) + k_{off}k_{12}} \quad \text{(A3)}$$

Equation A1, which expresses the initial steady state between regions 1 and 2, reflects the relationship between the ratio k_{21}/k_{12} and the initial probe concentrations in the two hemileaflets of the donor. Thus, for $k_{12} = k_{21}$, $C_1(0) = C_2(0)$.

In terms of these initial conditions, the solutions to eq 3–7 are

$$C_1(t) = C_2(0)k_{21}\{-[A]W_1 \exp(m_1t) - [A]W_2 \exp(m_2t) + [A]W_3 \exp(m_3t) + [A]W_4 \exp(m_4t) + II/k_{12}HH\} \quad \text{(A4)}$$

$$C_2(t) = C_2(0)\{Y_1 \exp(m_1t) + Y_2 \exp(m_2t) + [A]Y_3 \exp(m_3t) + [A]Y_4 \exp(m_4t) + II/HH\} \quad \text{(A5)}$$

$$C_3(t) = C_2(0)k_{off}[H_1 \exp(m_1t) + H_2 \exp(m_2t) + II/k_{on}]/[D]HH \quad \text{(A6)}$$

$$C_4(t) = C_2(0)[A]\{Y_1 \exp(m_1t)/[D] + Y_2 \exp(m_2t)/[D] - Y_3 \exp(m_3t) - Y_4 \exp(m_4t) + II/[D]HH\} \quad \text{(A7)}$$

$$C_5(t) = -C_2(0)k_{21}[A]\{W_1 \exp(m_1t)/[D] + W_2 \exp(m_2t)/[D] + W_3 \exp(m_3t) + W_4 \exp(m_4t) - II/[D]k_{12}HH\} \quad \text{(A8)}$$

The exponents in eq A4–A8 are

$$m_1 = (EE^{1/2} - BB)/2 \quad \text{(A9)}$$

$$m_2 = -(EE^{1/2} + BB)/2 \quad \text{(A10)}$$

$$m_3 = (CC^{1/2} - kkk)/2 \quad \text{(A11)}$$

$$m_4 = -(CC^{1/2} + kkk)/2 \quad \text{(A12)}$$

The preexponential factors in eq A4–A8 can be expressed as

$$W_1 = (k_{off}/2[T]HH)(1 + BB/EE^{1/2})$$

$$W_2 = (k_{off}/2[T]HH)(1 - BB/EE^{1/2})$$

$$W_3 = (1/2[T]k_{12})(1 + kkk/CC^{1/2})$$

$$W_4 = (1/2[T]k_{12})(1 - kkk/CC^{1/2})$$

$$Y_1 = -[A]k_{off}\{k_{12} - [2([T]k_{on}k_{21} - k_{12}(k_{12} + k_{21})) + k_{12}BB]/EE^{1/2}\}/2[T]HH$$

$$Y_2 = -[A]k_{off}\{k_{12} + [2([T]k_{on}k_{21} - k_{12}(k_{12} + k_{21})) + k_{12}BB]/EE^{1/2}\}/2[T]HH$$

$$Y_3 = (1/2[T])\{1 + [2(k_{12} + k_{21}) - kkk]/CC^{1/2}\}$$

$$Y_4 = (1/2[T])\{1 - [2(k_{12} + k_{21}) - kkk]/CC^{1/2}\}$$

$$H_1 = ([A]/2)[JJ + (k_{12} + k_{21})]$$

$$H_2 = ([A]/2)[-JJ + (k_{12} + k_{21})]$$

The symbols used in these solutions are defined as [T] = [A] + [D] ([A] and [D] are the acceptor and donor lipid concentrations, respectively):

$$BB = [T]k_{on} + k_{off} + k_{12} + k_{21}$$

$$kkk = k_{off} + k_{21} + k_{12}$$

$$CC = k_{off}^2 + 2(k_{21} - k_{12})k_{off} + (k_{12} + k_{21})^2$$

$$EE = ([T]k_{on} + k_{off} - k_{21} - k_{12})^2 + 4k_{21}k_{off}$$

$$HH = [T]k_{on}(k_{12} + k_{21}) + k_{12}k_{off}$$

$$II = [D]k_{on}(k_{12} + k_{21}) + k_{12}k_{off}$$

$$JJ = [2(k_{21}k_{off} + (k_{12} + k_{21})^2) - BB(k_{21} + k_{12})]/EE^{1/2}$$

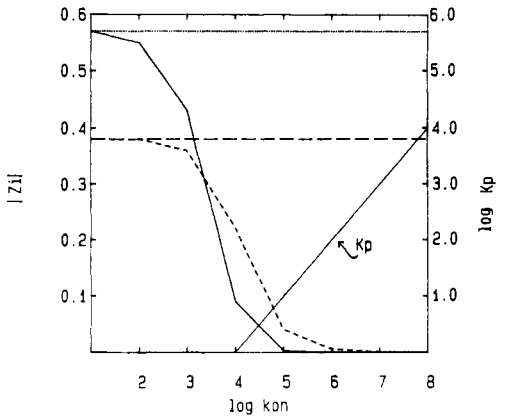

FIGURE 7: Effect of k_{on} variation on the kinetic model parameters Z_i and the lipid/water partition coefficient K_p. Symbols representing the preexponential factors Z_i of eq A9 are (···) Z_3, (– –) Z_4, (– · –) Z_2, (—) Z_1, and (thin line) K_p. K_p values are <1.0 for $k_{on} < 10^4$. These results demonstrate that for k_{on} values $>10^6$, Z_1 and Z_2 are less than 1%.

The observed fluorescence intensity normalized to unity at time = 0 is equal to $C_1(t) + C_2(t)/C_1(0) + C_2(0)$ and, therefore, in terms of eq A4 and A5 can be written as

$$F(t) = \sum_{i=1}^{4} Z_i \exp(m_i t) + C \qquad \text{(A13)}$$

in which

$$Z_3 = [\mathrm{A}](k_{21}W_3 + Y_3)/(1 + k_{21}/k_{12}) \qquad \text{(A14)}$$

$$Z_4 = [\mathrm{A}](k_{21}W_4 + Y_4)/(1 + k_{21}/k_{12}) \qquad \text{(A15)}$$

Although eq A13 involves four terms, the magnitudes only of Z_3 and Z_4 are significant for the rate constants encountered in lipid exchange. This is seen in Figure 7, where Z_i and K_p (the lipid/water partition coefficient) are plotted as a function of k_{on}. We have estimated from the rate of AOffa uptake that $k_{on} > 10^8$ M^{-1}, which agrees well with the values reported for phospholipids (Nichols & Pagano, 1981; Arvinte & Hildenbrand, 1984). Furthermore, since $K_p > 10^3$ (Pjura et al., 1984), it follows that the terms (with m_1 and m_2), which reflect back rate, contribute negligibly to the solutions of eq A4–A8.

Registry No. 12AD, 100334-39-2; 12AO, 73024-99-4; 2AP, 67708-96-7; 2AS, 78447-89-9; 3AS, 86637-08-3; 6AS, 67708-95-6; 9AS, 69243-44-3; 10AS, 56970-51-5; 12AS, 30536-60-8; 11AU, 73038-57-0; cholesterol, 57-88-5.

REFERENCES

Abumrad, N. A., Park, J. H., & Park, C. R. (1984) *J. Biol. Chem. 259*, 8945–8953.

Ando, S., Kon, K., & Tanaka, Y. (1980) in *Membrane Fluidity: Biophysical Techniques and Cellular Regulation* (Kates, M., & Kuksis, A., Eds.) pp 43–55, Humana Press, Clifton, NJ.

Arvinte, T., & Hildenbrand, K. (1984) *Biochim. Biophys. Acta 775*, 86–94.

Backer, J. M., & Dawidowicz, E. A. (1981) *Biochemistry 20*, 3805–3810.

Bevington, P. R. (1969) *Data Reduction and Error Analysis for the Physical Sciences*, McGraw-Hill, New York.

Brecher, P., Saouaf, R., Sugarman, J. M., Eisenberg, D., & LaRosa, K. (1984) *J. Biol. Chem. 259*, 13395–13401.

Carey, M. C., Small, D. M., & Bliss, C. M. (1983) *Annu. Rev. Physiol. 45*, 651–677.

Chalpin, D. B., & Kleinfeld, A. M. (1983) *Biochim. Biophys. Acta 731*, 465–474.

Charlton, S. C., & Smith, L. C. (1982) *Biochemistry 21*, 4623–4630.

Darke, A., Finer, E. G., Flook, A. G., & Phillips, M. C. (1972) *J. Mol. Biol. 63*, 265–279.

Demel, R. A., Van Kessel, W. S. M. G., & Van Deenen, L. L. M. (1972) *Biochim. Biophys. Acta 266*, 26–40.

Doody, M. C., Pownall, H. J., Kao, Y. J., & Smith, L. C. (1980) *Biochemistry 19*, 108–116.

Enoch, H. G., & Strittmatter, P. (1979) *Proc. Natl. Acad. Sci. U.S.A. 76*, 145–149.

Ferrell, J. E., Kong-Joo, L., & Huestis, W. H. (1985) *Biochemistry 24*, 2857–2864.

Gatt, S., Dinur, T., & Barenholz, Y. (1980) *Clin. Chem. (Winston-Salem, N.C.) 26*, 93–96.

Ginsburgh, C. L., Black, P. N., & Nunn, W. D. (1984) *J. Biol. Chem. 259*, 8437–8443.

Gomori, G. (1942) *J. Lab. Clin. Med. 27*, 955–960.

Hauser, H., Guyer, W., & Howell, K. (1979) *Biochemistry 18*, 3285–3291.

Huang, C., & Thompson, T. E. (1974) *Methods Enzymol. 32*, 485–489.

Keough, K. M., Oldfield, E., Chapman, D., & Beynon, P. (1973) *Chem. Phys. Lipids 10*, 37–50.

Kleinfield, A. M., Pandiscio, A. A., & Solomon, A. K. (1979) *Anal. Biochem. 94*, 65–74.

Kutchai, H., Chandler, L., & Zavoico, G. B. (1983) *Biochim. Biophys. Acta 736*, 137–149.

Maloy, S. R., Ginsburgh, C. L., Simons, R. W., & Nunn, W. D. (1981) *J. Biol. Chem. 256*, 3735–3742.

Martin, F. J., & McDonald, R. C. (1976) *Biochemistry 15*, 321–327.

Massey, J. B., Gotto, A. M., & Pownall, H. J. (1981) *J. Biol. Chem. 257*, 5444–5448.

Massey, J. B., Gotto, A. M., & Pownall, H. J. (1982) *Biochemistry 21*, 3630–3636.

Matayoshi, E. D., & Kleinfeld, A. M. (1981) *Biophys. J. 35*, 215–235.

McLean, L. R., & Phillips, M. C. (1981) *Biochemistry 20*, 2893–2900.

McLean, L. R., & Phillips, M. C. (1984) *Biochim. Biophys. Acta 776*, 21–26.

Miller, K. W., & Yu, S. (1977) *Br. J. Pharmacol. 61*, 57–63.

Monti, J. A., Christian, S. T., & Shaw, W. A. (1978) *J. Lipid Res. 19*, 222–228.

Morand, O., Fibach, E., Dagan, A., & Gatt, S. (1982) *Biochim. Biophys. Acta 711*, 539–550.

Nakagawa, T. (1974) *Colloid Polym. Sci. 252*, 56–64.

Nichols, J. W., & Pagano, R. E. (1981) *Biochemistry 20*, 2783–2789.

Nunn, W. D., Simons, R. W., Egan, P. A., & Maloy, S. R. (1979) *J. Biol. Chem. 254*, 9130–9134.

Phillips, M. C. (1972) *Prog. Surf. Membr. Sci. 5*, 139–221.

Pjura, W. J., Kleinfeld, A. M., & Karnovsky, M. J. (1984) *Biochemistry 23*, 2039–2043.

Pownall, H. J., Hickson, D., Gotto, A. M., & Massey, J. B. (1982) *Biochim. Biophys. Acta 712*, 169–176.

Pownall, H. J., Hickson, D., & Smith, L. C. (1983) *J. Am. Chem. Soc. 105*, 2440–2445.

Roseman, M. A., & Thompson, T. E. (1980) *Biochemistry 19*, 439–444.

Sengupta, P., Sackmann, E., Kuhnle, W., & Scholz, H. P. (1976) *Biochim. Biophys. Acta 436*, 869–878.

Shaklai, N., Yguerabide, J., & Ranney, H. M. (1977) *Biochemistry 16*, 5585–5592.

Sleight, R. G., & Pagano, R. E. (1985) *J. Biol. Chem. 260*, 1146–1154.
Storch, J., & Schachter, D. (1985) *Biochim. Biophys. Acta 812*, 473–484.
Stremmel, W., Lotz, G., Strohmeyer, G., & Berk, P. D. (1985) *J. Clin. Invest. 75*, 1068–1076.
Thilo, L. (1977) *Biochim. Biophys. Acta 469*, 326–334.
Thulborn, K. R., & Sawyer, W. H. (1978) *Biochim. Biophys. Acta 511*, 125–140.
Van Deenen, L. L. M. (1975) in *Biomembranes: Structure and Function* (Gordos, G., & Szasz, E., Eds.) North-Holland Publishing Co., Amsterdam.
Wolkowicz, P. E., Pownall, H. J., Pauly, D. F., & McMillan-Wood, J. B. (1984) *Biochemistry 23*, 6426–6432.

Activation of Porcine Pancreatic Phospholipase A_2 by the Presence of Negative Charges at the Lipid–Water Interface†

Johannes J. Volwerk,*,‡ Patricia C. Jost,‡,§ Gerard H. de Haas,‖ and O. Hayes Griffith‡

Institute of Molecular Biology, University of Oregon, Eugene, Oregon 97403, and Biochemical Laboratory, State University of Utrecht, Padualaan 8, 3508 TB-Utrecht, The Netherlands

Received March 18, 1985; Revised Manuscript Received November 8, 1985

ABSTRACT: The effect of surface charge on the porcine pancreatic phospholipase A_2 catalyzed hydrolysis of organized substrates was examined through initial rate enzyme kinetic measurements. Two long-chain phospholipid substrates, phosphatidylglycerol (PG) and phosphatidylcholine (PC), were solubilized in seven detergents differing in polar head-group charge. The neutral or zwitterionic detergents selected were Triton X-100, Zwittergent 314, lauryl maltoside, hexadecylphosphocholine (C_{16}PN), and 3-[(3-cholamidopropyl)dimethylammonio]-1-propanesulfonate. The negatively and positively charged detergents used were cholate and CTAB, respectively. In general, the negatively charged phospholipid PG was hydrolyzed much more rapidly than the neutral (zwitterionic) phospholipid PC. The rate of hydrolysis of PG was rapid when solubilized in all the neutral detergents and in cholate but was essentially zero in the positively charged CTAB. Conversely, hydrolysis of PC was negligible when solubilized in neutral detergents, except C_{16}PN, and was maximal in the negatively charged detergent, cholate. The rate of hydrolysis of PC solubilized in a neutral detergent became significant only when a negative surface charge was introduced by addition of SDS. Taken together, these kinetic measurements indicate that the surface charge on the lipid aggregates is an important factor in the rate of hydrolysis of phospholipid substrates and the highest activity is observed when the net surface charge is negative. Fluorescence and electron spin resonance (ESR) spectroscopic data provide additional support for this conclusion. The fluorescence emission spectrum of the single tryptophan of phospholipase A_2 is a sensitive monitor of interfacial complex formation and shows that interaction of the protein with detergent micelles is strongly dependent on the presence of a negatively charged amphiphile. Furthermore, ESR spectra of spin-labeled detergent analogues detect a significant decrease in lipid motion in the presence of protein only when the charge on the spin-label is negative.

Pancreatic phospholipase A_2 (EC 3.1.1.4) (PLA)[1] is a small water-soluble enzyme of M_r 14 000 that catalyzes the hydrolysis of the 2-acyl ester bond of 3-*sn*-phosphoglycerides. Primary sequences of more than 30 phospholipases A_2 isolated from mammalian pancreas and various snake venoms are known (Verheij et al., 1981). Three-dimensional structures of the porcine and bovine pancreatic enzymes as well as the enzyme from *Crotalus atrox* venom have been determined by X-ray crystallography (Dijkstra et al., 1981a, 1983; Keith et al., 1981). One of the most interesting aspects of phospholipase A_2, and one that distinguishes this enzyme from other water-soluble enzymes, is that it hydrolyzes substrates at a much higher rate when they are organized into larger aggregates such as micelles (Wells, 1972; Pieterson et al., 1974). Several models have been proposed to account for the interfacial activation of PLA and other lipolytic enzymes [reviewed by Volwerk & de Haas (1982)]. In the majority of kinetic studies on pancreatic as well as snake venom phospholipases, phospholipids carrying the neutral zwitterionic phosphocholine head group have been employed as substrates either as short-chain PC's in a single component system (de Haas et al., 1971; Wells, 1972) or as long-chain PC's mixed with uncharged detergents such as Triton X-100 (Dennis, 1973).

† This work was supported by U.S. Public Health Service Grant GM 25698.

‡ University of Oregon.
§ Present address: Biophysics Program, National Science Foundation, Washington, DC 20550.
‖ State University of Utrecht.

[1] Abbreviations: PLA, porcine pancreatic phospholipase A_2; PC, phosphatidylcholine; PG, phosphatidylglycerol; HETLC, high-efficiency thin-layer chromatography; C_{16}PN, *n*-hexadecylphosphocholine; Z314, *N*-tetradecyl-*N*,*N*-dimethyl-3-ammonio-1-propanesulfonate (Zwittergent 314); CHAPS, 3-[(3-cholamidopropyl)dimethylammonio]-1-propanesulfonate; CHOL, sodium cholate; OG, octyl glucoside; CTAB, cetyltrimethylammonium bromide; SDS, sodium dodecyl sulfate; TX100, Triton X-100; LM, lauryl maltoside; MP*, 14-proxylstearyl methyl phosphate sodium salt; QA*, (14-proxylstearyl)trimethylammonium mesylate; cmc, critical micelle concentration; TEM, transmission electron microscopy; Tris-HCl, tris(hydroxymethyl)aminomethane hydrochloride.

0006-2960/86/0425-1726$01.50/0